IAI Accepts, published online ahead of print on 5 July 2011
Infect. Immun. doi:10.1128/IAI.05175-11

Cholesterol depletion reduces entry of *Campylobacter jejuni* cytolethal distending toxin and attenuates intoxication of host cells

Running title: Cholesterol is essential for *C. jejuni* CDT intoxication

Chia-Der Lin,[1] Cheng-Kuo Lai,[2†] Yu-Hsin Lin,[3] Jer-Tsong Hsieh,[4] Yu-Ting Sing,[1] Yun-Chieh Chang,[5] Kai-Chuan Chen,[6] Wen-Ching Wang,[5] Hong-Lin Su,[2] and Chih-Ho Lai[1,4]*

School of Medicine and Graduate Institute of Basic Medical Science, China Medical University, Taichung, Taiwan[1]

Department of Life Sciences, National Chung Hsing University, Taichung, Taiwan[2]

Department of Biological Science and Technology, China Medical University, Taichung, Taiwan[3]

Department of Urology, University of Texas Southwestern Medical Center, Dallas, Texas, USA[4]

Institute of Molecular and Cellular Biology, National Tsing Hua University, Hsinchu, Taiwan[5]

Institute of Biomedical Sciences, Academia Sinica, Taipei, Taiwan[6]

[†] *Co-first author.*

Corresponding author. Mail address:

Chih-Ho Lai, PhD

School of Medicine and Graduate Institute of Basic Medical Science

China Medical University

No. 91 Hsueh-Shih Road, Taichung, 40402 Taiwan

Phone: 886-4-22052121 ext 7729

Fax: 886-4-22333641

E-mail: chl@mail.cmu.edu.tw

ABSTRACT

Campylobacter jejuni is a common cause of pediatric diarrhea worldwide. Cytolethal distending toxin, produced by *Campylobacter jejuni*, is a putative virulence factor that induces cell-cycle arrest and apoptosis in eukaryotic cells. Cellular cholesterol, a major component of lipid rafts, has a pivotal role in regulating signaling transduction and protein trafficking as well as pathogen internalization. In this study, we demonstrated that cell intoxication by *Campylobacter jejuni* cytolethal distending toxin is through the association of cytolethal distending toxin subunits and membrane cholesterol-rich microdomains. Cytolethal distending toxin subunits co-fractionated with detergent-resistant membranes, while the distribution reduced upon depletion of cholesterol, suggesting that cytolethal distending toxin subunits are associated with lipid rafts. Disruption of cholesterol using methyl-β-cyclodextrin not only reduced the binding activity of cytolethal distending toxin subunits on the cell membrane but also impaired their delivery and attenuated toxin-induced cell-cycle arrest. Accordingly, cell intoxication by cytolethal distending toxin was restored by cholesterol replenishment. These findings suggest that membrane cholesterol plays a critical role in *Campylobacter jejuni* cytolethal distending toxin-induced pathogenesis of host cells.

Keywords: *Campylobacter jejuni*, cytolethal distending toxin, cell cycle, cholesterol, lipid rafts

INTRODUCTION

Campylobacter jejuni is one of the most common causative agents of food-borne infectious illnesses in humans (10, 34). Inflammatory diarrhea is commonly seen in children infected with *Campylobacter* species (4, 47). Infection by the pathogen in humans usually occurs through the consumption of contaminated poultry products (13). However, the virulence factors responsible for the induction of host diarrhea remain unclear.

A bacterial membrane-associated protein, cytolethal distending toxin (CDT), has been identified as one of the virulence factors required for the induction of interleukin (IL)-8, which is a chemokine associated with local acute inflammatory responses (20, 59). CDT is a tripartite protein toxin composed of 3 subunits, CdtA, CdtB, and CdtC (28), encoded by an operon comprising *cdtA*, *cdtB*, and *cdtC* (46). Several bacterial species have been identified that contain CDT toxin, including *Aggregatibacter actinomycetemcomitans* (55), *C. jejuni* (22), *Escherichia coli* (45), *Haemophilus ducreyi* (12), *Helicobacter hepaticus* (58), and *Shigella dysenteriae* (41). CDT holotoxin functions as an AB_2 toxin in which CdtA and CdtC form a binding (B) unit and CdtB is an active (A) unit (27). A previous study demonstrated that CdtA and CdtC can interact with the cell membrane and enable the translocation of the holotoxin across the cell membrane (38). In addition, the nuclear-translocated CdtB subunit exhibits type I deoxyribonuclease activity, which causes DNA damage resulted in cell-cycle arrest at the G2/M phase (26).

Functional studies of CdtA and CdtC are relatively limited compared with those of CdtB. CdtA

and CdtC adopt lectin-type structures that are homologous to ricin, a plant toxin (37, 38). The crystal structure of CDT from *H. ducreyi* revealed that it contains 2 important binding elements: an aromatic patch in CdtA and a deep groove at the interface of CdtA and CdtC (38). A structure-based mutagenesis study further demonstrated that mutations of the aromatic patch or groove impair toxin binding to the cell surface and reduce cell intoxication (39). Analysis of CDT from *A. actinomycetemcomitans* also revealed that CdtA and CdtC not only bind to the cell surface but are associated with membrane lipid rafts (5). Lipid rafts are microdomains that contain large fractions of cholesterol, phospholipids, and glycosylphosphatidylinositol-anchored proteins (9, 21). *In vitro* studies showed that the structure of lipid rafts is stabilized in cold non-ionic detergents such as Triton X-100 (8), but can be disrupted by the cholesterol depletion agent methyl-β-cyclodextrin (MβCD) (54). A recent study of *A. actinomycetemcomitans* CDT revealed that the CdtC subunit contains a cholesterol recognition/interaction amino acid consensus (CRAC) region, which is required for CdtC binding to cholesterol-rich microdomains (6). This finding indicates that cholesterol provides an essential ligand for CDT binding to the cell membrane and also serves as a portal for CdtB delivery into host cells for the induction of cell intoxication.

A growing number of studies have reported that some pathogens exploit lipid rafts for toxin delivery to induce host pathogenesis (1, 5, 19, 25, 48). However, the interaction between *C. jejuni* CDT subunits and membrane cholesterol-rich microdomains as well as the role of cholesterol in the CDT intoxication of host cells are largely unknown. In the present study, we propose that the association of

81 *C. jejuni* CDT subunits with the host membrane is mediated in a cholesterol-dependent manner.
82 Biochemical and cellular studies as well as confocal microscopy were used to explore the association of
83 CdtA and CdtC with membrane lipid rafts. The binding of CDT subunits to the cell membrane, nuclear
84 delivery of CdtB, and G2/M arrest were reduced when cellular cholesterol was depleted. Our results
85 provide evidence that membrane cholesterol plays an essential role in the binding of *C. jejuni* CDT
86 subunits to membrane rafts, which promotes the pathogenic events in host cells.

MATERIALS AND METHODS

Reagents and antibodies. Anti-His (His-probe) and anti-proliferating cell nuclear antigen (anti-PCNA) were purchased from Santa Cruz Biotechnology (Santa Cruz, CA). Anti-caveolin-1 and anti-transferrin receptor [(anti- CD71)] were purchased from BD Pharmingen (San Jose, CA). Anti-actin mouse monoclonal antibodies were purchased from Upstate Biotechnology (Lake Placid, NY). Alexa Fluor 647−conjugated anti-rabbit IgG, and DAPI were purchased from Molecular Probes (Invitrogen, Carlsbad, CA). ICRF-193 was purchased from Sigma-Aldrich (St. Louis, MO). MβCD, a cholesterol depletion agent which was commonly utilized to extract eukaryotic cholesterol from lipid rafts (53), was purchased from Sigma-Aldrich.

Bacterial and cell models. *C. jejuni* strain 7729 isolated from patients' feces was identified and deposited at the Chang Gung Memorial Hospital (Taoyuan, Taiwan) (57). The bacterial strain was grown on Brucella blood agar plates (Becton Dickinson, Franklin Lakes, NJ) supplemented with 10% sheep blood and 1.5% agar in a microaerophilic atmosphere at 37°C for 1 to 2 days. CHO-K1 cells (Chinese hamster ovary cells, CCL 61; American Type Culture Collection, Manassas, VA) and AGS cells (human gastric adenocarcinoma cells, CRL 1739) were cultured in F12 medium (HyClone, Logan, UT), COLO205 cells (Human colon adenocarcinoma cells, CCL 222), and Caco-2 (Human colon adenocarcinoma cells, HTB-37) were cultured in RPMI 1640 medium (Invitrogen). All of cell culture medium were supplemented with 10% FBS (HyClone) and penicillin and streptomycin (Invitrogen).

106

107 **Construction and protein purification of CDT subunits.** Recombinant His-tagged CDT
108 subunits were cloned following standard protocols. DNA fragments of *cdtA*, *cdtB*, and *cdtC* were
109 derived from PCR amplification of *C. jejuni* 7729 genomic DNA. The forward and reverse
110 oligonucleotide primers were cdtA-F (CATGCCATGGCTTGTTCTTCTAAATTTGAAAATGT) and
111 cdtA-R (CCGCTCGAGTCGTACCTCTCCTTGGCGATATA) for PCR amplification of the *cdtA*
112 sequence; cdtB-F (CATGCCATGGCTAATTTAGAAAATTTTAATGTTGGC) and cdtB-R
113 (CCGCTCGAGAAATTTTCTAAAATTTACTGGAAA) for *cdtB* sequence; cdtC-F
114 (CATGCCATGGCTACTCCTACTGGAGATTTGAAAGA) and cdtC-R (CCGCTCGAGTT
115 CTAAAGGGGTAGCACTG) for *cdtC* sequence. Each *cdt* fragment was inserted into pET21d
116 (Invitrogen, Carlsbad, CA) using *Nco*I and *Xho*I. Briefly, *cdtA* was amplified using primers cdtA-F and
117 cdtA-R by PCR at 95°C 10 min for one cycle; 35 cycles at 95°C for 1 min, 55°C for 1min, and 72°C
118 for 2 min; and a final extension 72°C for 20 min. The *Nco*I/*Xho*I fragment was then ligated with
119 pET21d to create the CdtA expression plasmid. Similar protocols were used to obtain the CdtB and
120 CdtC expression plasmids from *C. jejuni* 7729 using primer pairs: cdtB-F and -R, and cdtC-F and -R,
121 respectively. The PCR program used to amplify *cdtB* and *cdtC* were the same as *cdtA*. The nucleotide
122 sequence of each *cdt* constructs were verified using the ABI Prism Dye Terminator Cycle Sequencing
123 Ready Reaction kit (Perkin-Elmer Corp, Norwalk, CT) in an automated DNA sequencer (model 377-96;
124 Perkin-Elmer Corp). Sequence analysis was performed by the University of Wisconsin Genetics

125 Computer Group (Madison, WI) package. The GenBank (National Center for Biotechnology
126 Information) accession numbers for *cdtA* and *cdtC* are JF520784 and JF682840, respectively. *E. coli*
127 BL21-DE3 cells harboring either *cdtA, cdtB,* or *cdtC* expression plasmid was induced at OD_{600} of 0.8
128 by 0.5 mM of isopropyl β-D-thiogalactopyranoside (IPTG) at 37°C for 3 h. The expressed His-tagged
129 CdtA, CdtB, and CdtC fusion proteins were purified by metal affinity chromatography (Clontech,
130 Palo-Alto, CA) and assessed by SDS-PAGE.
131
132 **Generation of antiserum against each CDT subunit.** Each purified CDT subunit (1 μg) was
133 used to immunize a 6-week-old BALB/C mouse. All of the mice were purchased from the National
134 Laboratory Animal Center (Taipei, Taiwan). The mice were immunized at weeks 0, 2, 4, 6, 8, 10, and
135 12, and the titer of the antiserum was detected at weeks 7, 9, 11, and 13. Mice were maintained in the
136 animal center of China Medical University (Taichung, Taiwan). All procedures were performed
137 according to the "Guide for the Care and Use of Laboratory Animals" (National Research Council,
138 USA) and were approved by the animal experiment committee of China Medical University (Taichung,
139 Taiwan). The titers of antibodies against the CDT subunits in the serum were determined by
140 Enzyme-linked immunosorbent assay (ELISA). Ninety-six-well plates were coated with 500 ng of
141 purified recombinant CDT subunits and blocked with 2% BSA in TBS (0.1 M Tris-HCl pH 7.5, 0.03 M
142 NaCl). Serial dilutions of the antiserum (1:1,000, 1:2,000, 1:4,000, 1:8,000, and 1:16,000) in
143 TBS-Tween 20 were added to each well. Bound antibody was detected by HRP-conjugated secondary

144 antibodies (Invitrogen) and quantified by measuring the optical density at 450 nm after development
145 with the TMB substrate buffer system (Kirkegaard & Perry Laboratories, Gaithersburg, MD).
146
147 **SDS-PAGE and western blot analysis.** CDT holotoxin-treated cells were washed three times
148 with PBS and then boiled in SDS-PAGE sample buffer for 5 min. The samples were then resolved by
149 12% SDS-PAGE and transferred onto polyvinylidene difluoride membranes (Millipore, Billerica, MA).
150 The membranes were incubated with antiserum against each CDT subunit, and then incubated with
151 horseradish peroxidase (HRP)-conjugated secondary antibodies (Invitrogen). The proteins of interest
152 were visualized using the ECL Western Blotting Detection Reagents (GE Healthcare, Piscataway, NJ)
153 and detected using X-ray film (Kodak, Rochester, NY).
154
155 **Cytolethal distending phenotype.** CHO-K1 cells were cultured at 37°C for 20 h in six-well
156 plates containing F-12 medium supplemented with 10% FBS. After one wash with PBS, cells were
157 exposed to an individual recombinant CDT subunit (200 nM) or CDT holotoxin (200 nM each subunit)
158 for 48 h. The CDT-treated cells were observed using an inverted optical microscope (Carl Zeiss,
159 Göttingen, Germany).
160
161 **Flow cytometry analysis of cell cycle.** CHO-K1 cells treated with CDT holotoxin were analyzed
162 by flow cytometry. Cells were pretreated with MβCD (Sigma-Aldrich) for 1 h, washed, and exposed to

CDT holotoxin or an individual CDT subunit for an additional 48 h. Cells were harvested and fixed with ice-cold 70% ethanol for 1 h, and stained with 20 μg/ml propidium iodide (Sigma-Aldrich) containing 1 mg/ml RNase (Sigma-Aldrich) for 1 h. The stained cells were analyzed with an FACScalibur flow cytometer (Becton-Dickinson, San Jose, CA). The data were collected using 20,000 cells from each sample, and analyzed using Cell Quest software WinMDI (Verity Software House, Topsham, ME). All samples were examined in triplicates from at least three independent experiments; all the data are the representation of a typical experimental outcome.

Detection of cellular cholesterol and cell viability assay. To measure the cholesterol levels in total cell lysates or detergent-resistant membrane (DRM), CHO-K1 cells were treated with various concentrations of MβCD. After incubation at 37°C for the indicated periods, the treated cells were washed three times with PBS and then disrupted by ultrasonication (three 10-sec bursts at room temperature). The cholesterol content was then measured using an Amplex Red Cholesterol Assay Kit (Molecular Probes, Eugene, OR). The percentage of remaining cholesterol after pretreatment with MβCD was determined [(fluorescence of treated cells obtained from a standard curve/total fluorescence of untreated cells) × 100] as previous described (25). To test the influence of MβCD on cell viability, cells were incubated with various concentrations of MβCD at 37°C for 1 h. After that, cells were washed three times with PBS, and then incubated with fresh medium containing 10 μM lovastatin (Sigma-Aldrich) to inhibit cellular cholesterol biosynthesis. After incubation for further 24 h, the

viability of cells was then determined by using trypan blue exclusion assay. In brief, equal volumes of 0.2% trypan blue (Sigma-Aldrich) and cell suspension were mixed. A 10 µl of the mixture was placed on the hemocytometer for counting trypan blue-stained cells. A total of 300 cells in randomly selected fields were counted by a light microscope. The percentages of alive and dead cells were calculated: cell viability (%) = (live cell count/total cell count) x 100]. The analysis was examined in three independent studies, each conducted in duplicate.

Immunofluorescence labeling of CDT-treated cells. To visualize localization of CDT in cells, CHO-K1 cells (0.5×10^6) were seeded on coverslips in six-well plates and incubated for 20 h. Cells were cultured with an individual CDT subunit (200 nM) or CDT holotoxin (200 nM each subunit) at 11°C for 1 h to maintain the fluidity of cell membrane and to prevent internalization of cells (24). The cultured cells were then washed three times with PBS and fixed with 3.7% paraformaldehyde (Sigma-Aldrich) for 1 h. The cells were permeabilized with 0.1% Triton X-100 for 30 min and stained with anti-caveolin-1 antibody (BD Pharmingen) followed by stained with Alexa Fluor 647−conjugated anti-rabbit IgG (Molecular Probes). To label the individual CDT subunit, samples were incubated for 30 min with anti-CdtA, anti-CdtB, or anti-CdtC antiserum followed by fluorescein isothiocyanate (FITC)-conjugated AffiniPure goat anti-mouse IgG (Jackson ImmunoResearch, West Grove, PA). Samples were analyzed under a confocal laser scanning microscope (Zeiss LSM 510, Carl Zeiss, Göttingen, Germany) with a 100× objective (oil immersion, aperture 1.3). The distribution of

fluorescence intensity for each CDT subunit and Cav-1 was analyzed by ZEN software (Carl Zeiss) and schemed as line intensity histograms.

Isolation and analysis of DRM fraction. To isolate detergent-soluble and detergent-resistant fractions, CDT-treated cells were lysed with ice-cold TNE buffer (25 mM Tris-HCl, pH 7.5, 150 mM NaCl, 5 mM EDTA) containing 1% Triton X-100 and incubated on ice for 30 min. Cell lysates were centrifuged at 18,000 × *g* at 4°C for 30 min to separate the detergent-soluble and detergent-resistant fractions as described previously (53). Each fraction was then analyzed by western blot.

Isolation of nuclear fractions. To study the localization of CdtB in the nucleus of target cells, CHO-K1 cells were incubated in the presence or absence of 10 mM MβCD at 37°C. After 1 h, cells were exposed to CDT holotoxin at 37°C for the indicated periods. The nuclear proteins were then prepared using a nuclear extraction kit (Pierce, Rockford, IL). All protein concentrations were determined by colorimetric assay using the Bio-Rad assay kit (Bio-Rad, Hercules, CA). The isolated proteins (20 μg) from the nuclear fractions were then subjected to western blot for further analysis of CdtB localization.

Statistical analysis. The Student's *t*-test was used to calculate the statistical significance of experimental results between two groups. $P < 0.05$ was considered statistically significant.

RESULTS

Expression and functional analysis of recombinant *C. jejuni* CDT subunits. We first investigated the activity of recombinant *C. jejuni* CDT using Chinese hamster ovary (CHO-K1) cells. Each *C. jejuni* CDT subunit was cloned and expressed with a His-tag in *E. coli* BL21-DE3 cells. Recombinant CDT subunits were then purified and analyzed by SDS-PAGE (Fig. 1A). The purified recombinant CDT subunits were readily detected by western blot analysis using a monoclonal anti-His antibody (Fig. 1B). Western blotting was carried out to determine whether polyclonal antibodies generated against each subunit could recognize the individual CDT subunits when they were assembled and associated with cells. As shown in Fig. 1C, the individual recombinant CDT proteins were recognized by the respective polyclonal CDT antiserum (anti-CdtA, anti-CdtB, or anti-CdtC). Thus, the polyclonal antisera were further applied to investigate the association of the CDT subunits with cell membrane lipid rafts. To characterize the biological function of *C. jejuni* CDT holotoxin, we examined its ability to induce cell distention in CHO-K1 cells. Our results revealed that any individual recombinant CDT protein had no effect on the cell cycle or the morphology of CHO-K1 cells after co-culture for 48 h (Fig. 1D). However, upon exposure of the cells to CDT holotoxin (200 nM each subunit) for 48 h, cell cycle analysis showed G2/M arrest and light microscopy indicated cell distention (Fig. 2).

To test whether CDT has the ability to intoxicate other cell types, we employed 3 different cell lines (AGS, CHO-K1, and COLO205 cells) to determine the intoxication activity of CDT. Each cell

line was treated with various concentrations of CDT and the cell cycle distribution was analyzed by flow cytometry. As shown in Fig. 3A, CDT-induced cell cycle arrest at the G2/M phase in these 3 cell lines exhibited in a dose-dependent manner. The saturation dose of CDT in AGS was ~200 nM. In contrast, the saturation dose of CDT in CHO-K1 and COLO205 cell lines were even higher; it could be higher than 500 nM. It appeared that AGS cells were more sensitive to CDT than the other 2 cell lines. We then determined the binding activity of each CDT subunit to CHO-K1 cells by flow cytometry. CdtA bound to CHO-K1 cells at a saturation level of ~10 nM (Fig. 3B). The binding activity of CdtC was higher than CdtA at a saturation concentration of ~200 nM; however, CdtB showed no detectable binding activity to CHO-K1 cells. These results indicated that CdtA and CdtC have binding activity to CHO-K1 cells, while CdtB did not.

Cholesterol is required for the association of *C. jejuni* CDT with the cell membrane. To determine whether cholesterol is important for the association of the *C. jejuni* CDT subunits with the membrane, we evaluated the ability of MβCD to deplete cholesterol from cells and membrane rafts (also called the detergent-resistant membrane [DRM]). As shown in Fig. 4A, the cholesterol concentration in total cell lysates and the DRM was decreased as early as 10 min after treatment of CHO-K1 cells with 10 mM MβCD. Furthermore, the cholesterol levels of total cell lysates and the DRM were reduced in a dose-dependent manner by MβCD treatment for 1 h. The result showed that over 60% and 90% of the cellular and DRM cholesterol, respectively, was extracted when cells were

258 treated with 10 mM MβCD (Fig. 4B). We then examined the cytotoxic effect of various concentrations
259 of MβCD on CHO-K1 cells; the cells remained essentially viable even when they were treated with 20
260 mM MβCD for 1 h followed by incubation with lovastatin for further 24 h (Fig. 4C).

261 We then assessed the association of the CDT subunits with membrane rafts. CHO-K1 cells were
262 first incubated with 200 nM of the individual CDT subunits for 2 h at 4°C. Subsequently, the cells were
263 analyzed by flow cytometry for the presence of CDT proteins on the cell membrane. As shown in Fig. 5
264 (upper panel), CdtA and CdtC were associated with the cell membrane. The mean channel fluorescence
265 (MCF) for anti-CdtA and anti-CdtC antibodies was 42.4 and 130.0, respectively; however, the MCF for
266 anti-CdtB antibody was only 11.0. When CHO-K1 cells were pretreated with 10 mM MβCD for 1 h,
267 the MCF was reduced for both anti-CdtA (26.4) and anti-CdtC (32.1) antibodies (Fig. 5, lower panel);
268 however, the MCF of the anti-CdtB (10.2) antibody remained the similar level to the cells not treated
269 with MβCD. We then examined whether cholesterol depletion could impact on the binding of CDT
270 holotoxin to cells. Noticeably, comparing with the control CHO-K1 cells (Fig. 6, upper panel), the
271 pretreatment of CHO-K1 cells with MβCD reduced CDT holotoxin binding (Fig. 6, lower panel).
272 Taken together, these results indicate that both CdtA and CdtC are the key binding subunits to DRM
273 and the activity of CdtB in holotoxin depends on the binding activity of CdtA and CdtC.

274 We next analyzed the detergent solubility of membranes from CDT-treated cells to determine
275 whether recombinant *C. jejuni* CDT holotoxin could associate with lipid rafts. CHO-K1 cells were
276 exposed to CDT holotoxin (200 nM each subunit) for 2 h at 37°C. The cells were then collected and

277 treated with ice-cold 1% Triton X-100 for 30 min, followed by gentle centrifugation to separate the
278 DRM and soluble fractions. Western blot showed that a raft-associated protein, caveolin-1 (Cav-1), was
279 enriched in the DRM fraction (Fig. 7). In contrast, a non-raft-associated protein, CD71 (also known as
280 the transferrin receptor), was mainly distributed in the soluble fraction. The localization of CdtA and
281 CdtC were enriched in the DRM fraction of CHO-K1 cells rather than in the soluble fraction (Fig. 7).
282 When cells were exposed to CDT holotoxin, the majority of CdtB was associated with DRM fraction,
283 but a small portion of this protein was found in the soluble fraction. However, when cells were
284 incubated with CdtB alone, CdtB was not detected in the DRM or soluble fractions (data not shown).
285 These results were consistent with the data presented in Figs. 5 and 6, suggesting that the delivery of *C.*
286 *jejuni* CdtB requires the association of both CdtA and CdtC subunits with the membrane rafts in target
287 cells.
288
289 **Delivery of CdtB into cells requires the association of CdtA and CdtC with raft**
290 **microdomains.** We next used confocal microscopy to visualize whether the distribution of *C. jejuni*
291 CDT subunits is raft-associated. CHO-K1 cells were incubated with 200 nM of the individual CDT
292 subunits at 11°C for 1 h to maintain cell membrane fluidity and prevent internalization. The cells were
293 then stained with pre-immune serum and antiserum to CdtA, CdtB, or CdtC. The cells were then
294 exposed to an anti-caveolin-1 antibody to identify the membrane raft microdomains. As expected, there
295 was no signal for CDT subunits in untreated CHO-K1 cells, whereas caveolin-1 staining was observed

296 around the plasma membrane (Fig. 8, 1st row). When cells were treated with each of the CDT subunits
297 at 11°C for 1 h, CdtA (green, Fig. 8, 2nd row) and CdtC (green, Fig. 8, 4th row) co-localized with
298 caveolin-1 (red) on the plasma membrane. In contrast, no CdtB fluorescence could be detected on the
299 plasma membrane (Fig. 8, 3rd row). We then examined CDT holotoxin with confocal microscopy.
300 Imaging analyses showed that CdtA (Fig. 9A) and CdtC (Fig. 9C) co-localized with caveolin-1 (red). In
301 parallel, CdtB was associated with membrane rafts (Fig. 9B). Analysis of the distribution of
302 fluorescence showed that all 3 CDT subunits co-localized with the membrane raft marker caveolin-1,
303 (Fig. 9D, E, and F). These data were consistent with our findings for CDT binding activity using flow
304 cytometry (Figs. 5 and 6), indicating that CdtA and CdtC not only associate with the membrane but also
305 co-localize with the cholesterol-rich microdomains.

306 To further test whether CdtB transport to the host cells is dependent on the association of CdtA
307 and CdtC with membrane lipid rafts, cells were exposed to CDT holotoxin (200 nM each subunit) at
308 37°C for 1–6 h. As expected, we first observed the cytoplasmic distribution of CdtB (green) at 2 h then
309 a clear nuclear distribution after 6 h in cells without MβCD (Fig. 10A, upper panel). However, the
310 amount of CdtB-associated fluorescence detected at the nucleus was visibly reduced when the cells
311 were pretreated with 10 mM MβCD (Fig. 10A, lower panel). We then examined whether the nuclear
312 localization of CdtB was dependent on the presence of cholesterol. The cells were pre-treated with 10
313 mM MβCD for 1 h and then exposed to CDT holotoxin for 1–6 h at 37°C. As shown in Fig. 10B and C,
314 the nuclear localization of CdtB gradually increased with incubation time in control cells, but its

nuclear localization was almost completely blocked in cells with MβCD treatment. Taken together, these observations support a notion that the binding of *C. jejuni* CdtA and CdtC to lipid rafts is important for the delivery of CdtB to target cells.

Cholesterol depletion prevents CDT-induced cell-cycle arrest. To determine whether *C. jejuni* CDT-induced cell cycle arrest depended on membrane rafts, we investigated whether the integrity of cholesterol-rich microdomains is essential for CDT holotoxin-induced cell cycle arrest. Only 17% of CHO-K1 control cells were in G2/M phase reflecting normal cell cycle distribution (Fig. 11A). Cells incubated with 5 or 10mM MβCD at 37°C for 1 h did not alter the cell cycle distribution as the control cells (Fig. 11B and C). In the presence of 2 μg/mL ICRF-193, a DNA topoisomerase II inhibitor (3), 60% of cells were accumulated in G2/M (Fig. 11D), which was used a positive control for a typical cell cycle arrest.

By pre-treating CHO-K1 cells with 0, 5, or 10 mM MβCD at 37°C for 1 h, the cells were then incubated with CDT holotoxin for 48 h, after removal of MβCD, clearly, the number of cells arrested in G2/M decreased in a dose-dependent manner (Fig. 11E–G). Apparently, cholesterol depletion by MβCD, which disrupts the integrity of rafts, also diminishes the activity of CDT, leading to the reduction of G2/M arrest. Upon replenishment of cholesterol, the inhibitory effect of MβCD on CDT-induced G2/M arrest was reversed (Fig. 11H and I). Together, these results indicate that the presence of sufficient cholesterol in membrane raft microdomains is required for the activity of *C.*

334 *jejuni* CDT.

335 We further analyzed whether depletion of cholesterol affects CDT-induced cell cycle arrest at the
336 G2/M phase in other cell types. Three intestinal-derived cell lines (AGS, COLO205, and Caco-2 cells)
337 were employed in this study. Cells were pretreated with or without MβCD for 1 h then exposed to CDT
338 holotoxin (200 nM) for 48 h. When cells were incubated with CDT holotoxin, a significant higher
339 number of cell cycle arrested at G2/M was detected in CHO-K1, AGS, COLO205, and Caco-2 cells
340 (Fig. 12A). The number of cells arrested in G2/M was significantly decreased in CHO-K1, AGS,
341 COLO205, and Caco-2 cells upon pretreatment of cells with MβCD. We further assessed whether
342 depletion of membrane cholesterol affects the association of the CDT subunits with cell surface. Cells
343 were incubated with 200 nM of each CDT subunit and analyzed by flow cytometry for the binding of
344 CDT proteins on the cell membrane. As shown in Fig. 12B, CdtA and CdtC were associated with the
345 cell membrane in all tested cell lines, but CdtB was not. After pre-treating cells with MβCD, the
346 binding activity of CdtA and CdtC was reduced significantly in all tested cells. These results implicated
347 that cholesterol is important for the association and intoxication of *C. jejuni* CDT in host cells.
348 Apparently, this effect is not only observed in CHO-K1 cells but also in other cells.

349

DISCUSSION

This study provides evidence that the interaction of *C. jejuni* CdtA and CdtC with cholesterol-rich membrane microdomains is essential for the delivery of CdtB to target cells. The association of *C. jejuni* CDT subunits with membrane lipid rafts was investigated using flow cytometry and biochemical analyses. Our data indicated that both the CdtA and CdtC subunits, but not CdtB subunit, are capable of binding to the cell membrane, and this binding activity was reduced after cholesterol depletion by MβCD. The CdtB subunit alone neither bound to the cell surface nor associated with lipid rafts, in contrast, CdtB was identified in the DRM fraction from cells incubated with CDT holotoxin. These findings are consistent with the crystal structure of CDT from *H. ducreyi* (38, 39). CdtA and CdtC with a high homologous to ricin have been shown to have prominent molecular surfaces, an aromatic cluster and a deep groove, that contribute to their membrane interactions (38). Another report also indicated that the 3 CDT subunits from *A. actinomycetemcomitans* form a functional toxin unit on the cell surface, which requires the complex formation between the CdtA and CdtC subunits (51). These results indicate that the 3 subunits need to be assembled prior to holotoxin binding to the cell membrane. This is consistent with our observation that, in the presence of holotoxin, *C. jejuni* CdtB was detected predominantly in the DRM fraction of target cells and this interaction is likely mediated through the association of CdtA and CdtB with lipid rafts.

In this study, we first employed CHO-K1 to study the mechanism of action of CDT holotoxin. Many studies also used this model for analysis of CDT functions in *Campylobacter* spp. (2, 22, 36, 40),

A. actinomycetemcomitans (11, 31, 32), *Escherichia coli* (7, 43), and *Shigella dysenteriae* (41) for decades. Thus, it appears that CHO-K1 is a good model for delineating mechanisms of CDT. Nevertheless, we further employed 3 additional intestinal-derived cell lines (AGS, COLO205, and Caco-2 cells) to validate whether cholesterol plays a crucial role in the CDT binding and its activity. Our results conclude that depletion of cholesterol affects CDT function not only in CHO-K1 cells but also in other cell lines (Fig. 12).

The CRAC region contains the conserved motif $L/V(X)_{1–5}Y(X)_{1–5}R/K$, which is present in proteins that associate with cholesterol (29). A recent report showed that the CdtC subunit of *A. actinomycetemcomitans* contains a CRAC region, which may contribute to the interaction between CdtC and cholesterol (6). Our data and another study (5) indicated that CdtA and CdtC were mainly localized in the cholesterol-rich microdomains. We then analyzed the conserved region within the *C. jejuni* CdtC subunit (44), i.e., the amino acid sequence that represents a CRAC-like region (^{77}LPFGYVQFTNPK^{88}) (Fig. 13). Also, *C. jejuni* CdtA possesses a conserved CRAC-like motif (^{17}LYACSSK^{23}). Thus, these observations may indicate that *C. jejuni* CdtA and CdtC contain hypothetical CRAC regions that contribute to their cholesterol-binding activity. However, we did not demonstrate a direct interaction between CdtA/C and cholesterol. Moreover, not all proteins that bind cholesterol have CRAC domains. A recent report indicated that only 2 amino acids are responsible for the recognition of cholesterol by cytolysin (16). Certainly, further investigation is needed to determine whether the CRAC-like motifs are the most important regions for the interaction of *C. jejuni* CdtA and

CdtC with cholesterol.

The importance of cellular cholesterol for another CDT from *A. actinomycetemcomitans* has been well documented by Boesze-Battaglia and the colleagues (5). These authors used either confocal microscopy or flow cytometry analysis. Similarly, we also found that CdtA/C of *C. jejuni* could bind to cell membrane particularly in the raft microdomains, and this effect was responsible for its toxicity activity. However, we notice some differences of CDT between *A. actinomycetemcomitans* and *C. jejuni* from this study. For example, CDT from *A. actinomycetemcomitans* has been demonstrated that interacted with the glycosphingolipids GM1, GM2, and GM3 (35). CHO-K1 cells lack GM2 synthase, which is an upstream enzyme required for GM1 synthesis (49), suggesting that the binding of CDT from *C. jejuni* to the receptors in the cholesterol-enriched microdomains might be different from *A. actinomycetemcomitans*. Noticeably, in this study, we employed cell models resembling the natural host for *C. jejuni*. Therefore, we believe that the outcome of this study reflects the physiological relevance of this toxin.

Several studies have reported that lipid rafts might serve as an entry site for pathogens. For instance, in *Shigella flexneri,* the bacterial invasin IpaB interacts with raft-associated CD44 within specialized membrane microdomains (24). Type 1-fimbriated *E. coli* was also found to be associated with caveolae and lipid raft components (14). Bacteria hijack lipid rafts to mediate the infectious process; similarly, lipid rafts are required for the translocation of cytotoxin-associated gene A (CagA) as well as for the delivery of vacuolating cytotoxin (VacA) into host cells following *H. pylori* infection

407 (17, 23, 25, 50). These results suggest that lipid rafts are not only a dynamic structure on the cell
408 membrane but also provide a bacterial entry site for toxin delivery into target cells. Our study suggests
409 that the association of CdtA and CdtC with membrane rafts mediates the action of the toxin more
410 efficiently. This idea is supported by the finding that the *A. actinomycetemcomitans* CdtB subunit
411 exhibits phophatidylinositol-3,4,5-triphosphate (PIP3) phosphatase activity similar to that of
412 phosphatase and tensin homolog deleted on chromosome 10 (PTEN) (30, 52). A previous study found
413 that PTEN normally has a generalized cytosolic and membrane distribution, but is recruited into
414 membrane rafts when cells are treated with ceramide (18). We found that both CdtA and CdtC interact
415 with lipid rafts (predominantly localized in cholesterol-rich microdomains) to enhance the association
416 of CdtB with the cell membrane and its subsequent delivery into the cells. This association may be
417 important for the toxin to hijack lipid rafts for the regulation of PIP3 signaling and thereby increase the
418 efficiency of cell intoxication.

419 In a recent report, Eshraghi *et al.* presented a comprehensive analysis of the role of glycosylation
420 and cholesterol on the ability of CDTs from several bacterial species, including *A.*
421 *actinomycetemcomitans*, *C. jejuni*, *E. coli*, and *H. ducreyi*, to intoxicate different cell types (15). The
422 authors found that CDT from *C. jejuni*-induced CHO-K1 cell intoxication was much less efficient than
423 the intoxication of CHO-K1 cells with other CDTs or the intoxication of other cell types with *C. jejuni*
424 CDT. The authors also demonstrated that *C. jejuni* CDT-induced cell cycle arrest of CHO-K1 cells was
425 not influenced by cholesterol loading, but was enhanced by inhibiting glycosylation. In contrast, in this

426 study, we showed that cholesterol plays a crucial role in the binding of *C. jejuni* CDT with CHO-K1
427 cells. This discrepancy may be due to the different concentrations of *C. jejuni* CDT used in these
428 studies. We applied a higher concentration of *C. jejuni* CDT (200 nM) than Eshraghi's study (50 nM) in
429 which cell cycle arrest in CHO-K1 cells became more apparent under the higher concentration of CDT,
430 suggesting that higher concentration of CDT may be mediated through different mechanisms.
431 Additionally, we used MβCD to deplete cholesterol from lipid rafts and showed the reduced binding
432 activity of CdtA and CdtC, which is different from Eshraghi *et al*., adding cholesterol directly into
433 cultured cells. Another key question is the specificity of MβCD to cholesterol. Depletion of cholesterol
434 by MβCD may also have extracted other raft-associated molecules, e.g., glycoproteins and gangliosides
435 (42, 53, 56). A previous study indicated that carbohydrate residues might be important for CDT binding
436 to cells (33). It is reasonable to speculate that receptor candidates may be removed after treating cells
437 with MβCD; thus, this may explain the influence of MβCD treatment on the cell binding activity of
438 CdtA and CdtC observed in our study.

439 In conclusion, we demonstrated that membrane cholesterol plays a critical role in *C. jejuni* CDT
440 intoxication of cells and CdtA and CdtC were associated with lipid rafts, which are critical for the
441 delivery of CdtB into target cells. Modulation of cellular cholesterol levels may reduce the association
442 of *C. jejuni* CDT with rafts, thereby attenuating CDT-induced pathogenesis of host cells. The precise
443 molecular mechanism by which CdtA and CdtC interact with cholesterol-rich microdomains will be the
444 subject of future studies. Since CDT is present in various bacterial species, investigation of the

445 molecular mechanisms underlying cell cycle arrest and eventual death by *C. jejuni* CDT will advance
446 the understanding of the pathogenicity of CDT-producing bacteria. Very likely, this outcome will
447 enhance the development of novel therapeutic strategies to prevent or cure diseases caused by these
448 bacterial pathogens.
449

ACKNOWLEDGMENTS

This work was supported by the National Science Council, Taiwan (NSC97-2313-B-039-003-MY3, NSC100-2918-I-039-003), China Medical University, Taiwan (CMU98-S-09, CMU98-CT-12), and the Tomorrow Medical Foundation, Taiwan. The authors thank Drs. Tsu-Lan Wu and Ju-Hsin Chia (Department of Laboratory Medicines, Chang Gung Memorial Hospital, Taoyuan, Taiwan) for kindly providing *C. jejuni*, and Drs. Wan-Chi Lee, Yu-Lun Lu, Pan-Cien Hsu, and Ming-Chun Kuo for expert technical assistance.

DISCLOSURE STATEMENT: all authors have no conflicts of interest to declare for this work.

References

1. **Abrami, L., S. Liu, P. Cosson, S. H. Leppla, and F. G. van der Goot.** 2003. Anthrax toxin triggers endocytosis of its receptor via a lipid raft-mediated clathrin-dependent process. J. Cell Biol. **160:**321-328.

2. **Bag, P. K., T. Ramamurthy, and U. B. Nair.** 1993. Evidence for the presence of a receptor for the cytolethal distending toxin (CLDT) of *Campylobacter jejuni* on CHO and HeLa cell membranes and development of a receptor-based enzyme-linked immunosorbent assay for detection of CLDT. FEMS Microbiol. Lett. **114:**285-291.

3. **Baus, F., V. Gire, D. Fisher, J. Piette, and V. Dulic.** 2003. Permanent cell cycle exit in G2 phase after DNA damage in normal human fibroblasts. EMBO J. **22:**3992-4002.

4. **Blaser, M. J., R. E. Black, D. J. Duncan, and J. Amer.** 1985. *Campylobacter jejuni*-specific serum antibodies are elevated in healthy Bangladeshi children. J. Clin. Microbiol. **21:**164-167.

5. **Boesze-Battaglia, K., D. Besack, T. McKay, A. Zekavat, L. Otis, K. Jordan-Sciutto, and B. J. Shenker.** 2006. Cholesterol-rich membrane microdomains mediate cell cycle arrest induced by *Actinobacillus actinomycetemcomitans* cytolethal-distending toxin. Cell. Microbiol. **8:**823-836.

6. **Boesze-Battaglia, K., A. Brown, L. Walker, D. Besack, A. Zekavat, S. Wrenn, C. Krummenacher, and B. J. Shenker.** 2009. Cytolethal distending toxin-induced cell cycle arrest of lymphocytes is dependent upon recognition and binding to cholesterol. J. Biol. Chem. **284:**10650-10658.

7. **Bouzari, S., and A. Varghese.** 1990. Cytolethal distending toxin (CLDT) production by enteropathogenic *Escherichia coli* (EPEC). FEMS Microbiol. Lett. **59:**193-198.

8. **Brown, D., and G. L. Waneck.** 1992. Glycosyl-phosphatidylinositol-anchored membrane proteins. J. Am. Soc. Nephrol. **3:**895-906.

9. **Brown, D. A., and E. London.** 1998. Functions of lipid rafts in biological membranes. Annu. Rev. Cell Dev. Biol. **14:**111-136.

10. **Butzler, J. P., and M. B. Skirrow.** 1979. Campylobacter enteritis. Clin Gastroenterol **8:**737-765.

11. **Cao, L., A. Volgina, C. M. Huang, J. Korostoff, and J. M. DiRienzo.** 2005. Characterization of point mutations in the *cdtA* gene of the cytolethal distending toxin of *Actinobacillus actinomycetemcomitans*. Mol. Microbiol. **58:**1303-1321.

12. **Cope, L. D., S. Lumbley, J. L. Latimer, J. Klesney-Tait, M. K. Stevens, L. S. Johnson, M. Purven, R. S. Munson, Jr., T. Lagergard, J. D. Radolf, and E. J. Hansen.** 1997. A diffusible cytotoxin of *Haemophilus ducreyi*. Proc. Natl. Acad. Sci. USA **94:**4056-4061.

13. **Corry, J. E., and H. I. Atabay.** 2001. Poultry as a source of *Campylobacter* and related organisms. Symp. Ser. Soc. Appl. Microbiol. **:**96S-114S.

14. **Duncan, M. J., G. Li, J. S. Shin, J. L. Carson, and S. N. Abraham.** 2004. Bacterial penetration of bladder epithelium through lipid rafts. J. Biol. Chem. **279:**18944-18951.

15. **Eshraghi, A., F. J. Maldonado-Arocho, A. Gargi, M. M. Cardwell, M. G. Prouty, S. R. Blanke, and K. A. Bradley.** 2010. Cytolethal distending toxin family members are differentially affected

by alterations in host glycans and membrane cholesterol. J. Biol. Chem. **285:**18199-18207.

16. **Farrand, A. J., S. LaChapelle, E. M. Hotze, A. E. Johnson, and R. K. Tweten.** 2010. Only two amino acids are essential for cytolytic toxin recognition of cholesterol at the membrane surface. Proc. Natl. Acad. Sci. USA **107:**4341-4346.

17. **Gauthier, N. C., P. Monzo, V. Kaddai, A. Doye, V. Ricci, and P. Boquet.** 2005. *Helicobacter pylori* VacA cytotoxin: a probe for a clathrin-independent and Cdc42-dependent pinocytic pathway routed to late endosomes. Mol. Biol. Cell **16:**4852-4866.

18. **Goswami, R., D. Singh, G. Phillips, J. Kilkus, and G. Dawson.** 2005. Ceramide regulation of the tumor suppressor phosphatase PTEN in rafts isolated from neurotumor cell lines. J. Neurosci. Res. **81:**541-550.

19. **Guerra, L., K. Teter, B. N. Lilley, B. Stenerlow, R. K. Holmes, H. L. Ploegh, K. Sandvig, M. Thelestam, and T. Frisan.** 2005. Cellular internalization of cytolethal distending toxin: a new end to a known pathway. Cell. Microbiol. **7:**921-934.

20. **Hickey, T. E., A. L. McVeigh, D. A. Scott, R. E. Michielutti, A. Bixby, S. A. Carroll, A. L. Bourgeois, and P. Guerry.** 2000. *Campylobacter jejuni* cytolethal distending toxin mediates release of interleukin-8 from intestinal epithelial cells. Infect. Immun. **68:**6535-6541.

21. **Hooper, N. M.** 1999. Detergent-insoluble glycosphingolipid/cholesterol-rich membrane domains, lipid rafts and caveolae (review). Mol. Membr. Biol. **16:**145-156.

22. **Johnson, W. M., and H. Lior.** 1988. A new heat-labile cytolethal distending toxin (CLDT)

produced by *Campylobacter* spp. Microb. Pathog. **4:**115-126.

23. **Kuo, C. H., and W. C. Wang.** 2003. Binding and internalization of *Helicobacter pylori* VacA via cellular lipid rafts in epithelial cells. Biochem. Biophys. Res. Commun. **303:**640-644.

24. **Lafont, F., G. Tran Van Nhieu, K. Hanada, P. Sansonetti, and F. G. van der Goot.** 2002. Initial steps of *Shigella* infection depend on the cholesterol/sphingolipid raft-mediated CD44-IpaB interaction. EMBO J. **21:**4449-4457.

25. **Lai, C. H., Y. C. Chang, S. Y. Du, H. J. Wang, C. H. Kuo, S. H. Fang, H. W. Fu, H. H. Lin, A. S. Chiang, and W. C. Wang.** 2008. Cholesterol depletion reduces *Helicobacter pylori* CagA translocation and CagA-induced responses in AGS cells. Infect. Immun. **76:**3293-3303.

26. **Lara-Tejero, M., and J. E. Galan.** 2000. A bacterial toxin that controls cell cycle progression as a deoxyribonuclease I-like protein. Science **290:**354-357.

27. **Lara-Tejero, M., and J. E. Galan.** 2001. CdtA, CdtB, and CdtC form a tripartite complex that is required for cytolethal distending toxin activity. Infect. Immun. **69:**4358-4365.

28. **Lara-Tejero, M., and J. E. Galan.** 2002. Cytolethal distending toxin: limited damage as a strategy to modulate cellular functions. Trends. Microbiol. **10:**147-152.

29. **Li, H., and V. Papadopoulos.** 1998. Peripheral-type benzodiazepine receptor function in cholesterol transport. Identification of a putative cholesterol recognition/interaction amino acid sequence and consensus pattern. Endocrinology **139:**4991-4997.

30. **Maehama, T., and J. E. Dixon.** 1999. PTEN: a tumour suppressor that functions as a

phospholipid phosphatase. Trends Cell Biol. **9:**125-128.

31. **Mao, X., and J. M. DiRienzo.** 2002. Functional studies of the recombinant subunits of a cytolethal distending holotoxin. Cell. Microbiol. **4:**245-255.

32. **Mayer, M. P., L. C. Bueno, E. J. Hansen, and J. M. DiRienzo.** 1999. Identification of a cytolethal distending toxin gene locus and features of a virulence-associated region in *Actinobacillus actinomycetemcomitans*. Infect. Immun. **67:**1227-1237.

33. **McSweeney, L. A., and L. A. Dreyfus.** 2005. Carbohydrate-binding specificity of the *Escherichia coli* cytolethal distending toxin CdtA-II and CdtC-II subunits. Infect. Immun. **73:**2051-2060.

34. **Mead, P. S., L. Slutsker, V. Dietz, L. F. McCaig, J. S. Bresee, C. Shapiro, P. M. Griffin, and R. V. Tauxe.** 1999. Food-related illness and death in the United States. Emerg. Infect. Dis. **5:**607-625.

35. **Mise, K., S. Akifusa, S. Watarai, T. Ansai, T. Nishihara, and T. Takehara.** 2005. Involvement of ganglioside GM3 in G(2)/M cell cycle arrest of human monocytic cells induced by *Actinobacillus actinomycetemcomitans* cytolethal distending toxin. Infect. Immun. **73:**4846-4852.

36. **Mizuno, K., K. Takama, and S. Suzuki.** 1994. Characteristics of cytotoxin produced by *Campylobacter jejuni* strains. Microbios. **78:**215-228.

37. **Montfort, W., J. E. Villafranca, A. F. Monzingo, S. R. Ernst, B. Katzin, E. Rutenber, N. H. Xuong, R. Hamlin, and J. D. Robertus.** 1987. The three-dimensional structure of ricin at 2.8 A. J. Biol. Chem. **262:**5398-5403.

38. **Nesic, D., Y. Hsu, and C. E. Stebbins.** 2004. Assembly and function of a bacterial genotoxin.

Nature **429:**429-433.

39. **Nesic, D., and C. E. Stebbins.** 2005. Mechanisms of assembly and cellular interactions for the bacterial genotoxin CDT. PLoS Pathog **1:**e28.

40. **Ohya, T., K. Tominaga, and M. Nakazawa.** 1993. Production of cytolethal distending toxin (CLDT) by *Campylobacter fetus* subsp. fetus isolated from calves. J. Vet. Med. Sci. **55:**507-509.

41. **Okuda, J., H. Kurazono, and Y. Takeda.** 1995. Distribution of the *cytolethal distending toxin A gene* (*cdtA*) among species of *Shigella* and *Vibrio*, and cloning and sequencing of the *cdt* gene from *Shigella dysenteriae*. Microb. Pathog. **18:**167-172.

42. **Orlandi, P. A., and P. H. Fishman.** 1998. Filipin-dependent inhibition of cholera toxin: evidence for toxin internalization and activation through caveolae-like domains. J. Cell Biol. **141:**905-915.

43. **Orth, D., K. Grif, M. P. Dierich, and R. Wurzner.** 2006. Cytolethal distending toxins in Shiga toxin-producing *Escherichia coli*: alleles, serotype distribution and biological effects. J. Med. Microbiol. **55:**1487-1492.

44. **Parkhill, J., B. W. Wren, K. Mungall, J. M. Ketley, C. Churcher, D. Basham, T. Chillingworth, R. M. Davies, T. Feltwell, S. Holroyd, K. Jagels, A. V. Karlyshev, S. Moule, M. J. Pallen, C. W. Penn, M. A. Quail, M. A. Rajandream, K. M. Rutherford, A. H. van Vliet, S. Whitehead, and B. G. Barrell.** 2000. The genome sequence of the food-borne pathogen *Campylobacter jejuni* reveals hypervariable sequences. Nature **403:**665-668.

45. **Peres, S. Y., O. Marches, F. Daigle, J. P. Nougayrede, F. Herault, C. Tasca, J. De Rycke, and**

E. Oswald. 1997. A new cytolethal distending toxin (CDT) from *Escherichia coli* producing CNF2 blocks HeLa cell division in G2/M phase. Mol. Microbiol. **24:**1095-1107.

46. **Pickett, C. L., E. C. Pesci, D. L. Cottle, G. Russell, A. N. Erdem, and H. Zeytin.** 1996. Prevalence of cytolethal distending toxin production in *Campylobacter jejuni* and relatedness of *Campylobacter* sp. *cdtB* gene. Infect. Immun. **64:**2070-2078.

47. **Rasrinaul, L., O. Suthienkul, P. D. Echeverria, D. N. Taylor, J. Seriwatana, A. Bangtrakulnonth, and U. Lexomboon.** 1988. Foods as a source of enteropathogens causing childhood diarrhea in Thailand. Am. J. Trop. Med. Hyg. **39:**97-102.

48. **Ricci, V., A. Galmiche, A. Doye, V. Necchi, E. Solcia, and P. Boquet.** 2000. High cell sensitivity to *Helicobacter pylori* VacA toxin depends on a GPI-anchored protein and is not blocked by inhibition of the clathrin-mediated pathway of endocytosis. Mol. Biol. Cell **11:**3897-3909.

49. **Rosales Fritz, V. M., J. L. Daniotti, and H. J. Maccioni.** 1997. Chinese hamster ovary cells lacking GM1 and GD1a synthesize gangliosides upon transfection with human GM2 synthase. Biochim. Biophys. Acta. **1354:**153-158.

50. **Schraw, W., Y. Li, M. S. McClain, F. G. van der Goot, and T. L. Cover.** 2002. Association of *Helicobacter pylori* vacuolating toxin (VacA) with lipid rafts. J. Biol. Chem. **277:**34642-34650.

51. **Shenker, B. J., D. Besack, T. McKay, L. Pankoski, A. Zekavat, and D. R. Demuth.** 2005. Induction of cell cycle arrest in lymphocytes by *Actinobacillus actinomycetemcomitans* cytolethal distending toxin requires three subunits for maximum activity. J. Immunol. **174:**2228-2234.

52. **Shenker, B. J., M. Dlakic, L. P. Walker, D. Besack, E. Jaffe, E. LaBelle, and K. Boesze-Battaglia.** 2007. A novel mode of action for a microbial-derived immunotoxin: the cytolethal distending toxin subunit B exhibits phosphatidylinositol 3,4,5-triphosphate phosphatase activity. J. Immunol. **178:**5099-5108.

53. **Simons, K., and D. Toomre.** 2000. Lipid rafts and signal transduction. Nat. Rev. Mol. Cell Biol. **1:**31-39.

54. **Simons, M., E. M. Kramer, P. Macchi, S. Rathke-Hartlieb, J. Trotter, K. A. Nave, and J. B. Schulz.** 2002. Overexpression of the myelin proteolipid protein leads to accumulation of cholesterol and proteolipid protein in endosomes/lysosomes: implications for Pelizaeus-Merzbacher disease. J. Cell Biol. **157:**327-336.

55. **Sugai, M., T. Kawamoto, S. Y. Peres, Y. Ueno, H. Komatsuzawa, T. Fujiwara, H. Kurihara, H. Suginaka, and E. Oswald.** 1998. The cell cycle-specific growth-inhibitory factor produced by *Actinobacillus actinomycetemcomitans* is a cytolethal distending toxin. Infect. Immun. **66:**5008-5019.

56. **Wolf, A. A., M. G. Jobling, S. Wimer-Mackin, M. Ferguson-Maltzman, J. L. Madara, R. K. Holmes, and W. I. Lencer.** 1998. Ganglioside structure dictates signal transduction by cholera toxin and association with caveolae-like membrane domains in polarized epithelia. J. Cell Biol. **141:**917-927.

57. **Wu, T. L., L. H. Su, J. H. Chia, T. M. Kao, C. H. Chiu, A. J. Kuo, and C. F. Sun.** 2002.

612 Molecular epidemiology of nalidixic acid-resistant campylobacter isolates from humans and
613 poultry by pulsed-field gel electrophoresis and flagellin gene analysis. Epidemiol. Infect.
614 **129:**227-231.
615 58. **Young, V. B., K. A. Knox, and D. B. Schauer.** 2000. Cytolethal distending toxin sequence and
616 activity in the enterohepatic pathogen *Helicobacter hepaticus*. Infect. Immun. **68:**184-191.
617 59. **Zheng, J., J. Meng, S. Zhao, R. Singh, and W. Song.** 2008. Campylobacter-induced
618 interleukin-8 secretion in polarized human intestinal epithelial cells requires
619 Campylobacter-secreted cytolethal distending toxin- and Toll-like receptor-mediated activation of
620 NF-kappaB. Infect. Immun. **76:**4498-4508.
621

FIGURE LEGENDS

FIG. 1. Purification and characterization of each recombinant *C. jejuni* CDT subunit. (A) CDT proteins were expressed and purified as described in the MATERIALS AND METHODS. Each CDT subunit (2 μg/mL) was subjected to SDS-PAGE and stained with Coomassie brilliant blue. (B) Recombinant CDT protein (2 μg/mL) was loaded into each lane and verified by western blot analysis with a monoclonal antibody specific to the His-tag. (C) Western blot analysis was conducted on extracts of CHO-K1 cells exposed to the CDT holotoxin and assessed by antisera against CdtA, CdtB, or CdtC. Molecular weight markers (kDa) are shown on the left. (D) CHO-K1 cells were untreated (control) or treated with 200 nM of each purified recombinant subunit at 37°C for 48 h. The cells were then examined under an inverted optical microscope to assess the effects of each CDT subunit. The cell cycle distribution was based on the DNA content, which was determined by flow cytometry. The percentage of cells in the G0/G1, S, and G2/M phases of the cell cycle are indicated below the insets. Scale bar, 50 μm. The results represent 1 of 3 independent experiments.

FIG. 2. Cell-distending activity of recombinant *C. jejuni* CDT subunits in CHO-K1 cells. CHO-K1 cells were untreated (A) or treated (B) with *C. jejuni* CDT holotoxin (CdtA, B, or C, 200 nM each subunit) for 48 h at 37°C. The cells were then examined under an inverted optical microscope to assess the effects of CDT intoxication. Scale bar, 100 μm. The cell cycle distribution was based on the DNA content, which was determined by flow cytometry. The percentage of cells in the G0/G1, S, and

642 G2/M phases of the cell cycle are indicated below the insets. The results represent 1 of 3 independent
643 experiments.
644
645 **FIG. 3.** CDT intoxication and binding of cells. (A) Cells from the indicated lines were treated with
646 various concentrations of CDT holotoxin (0.01–500 nM) and incubated at 37°C for 48 h. Cell cycle
647 distribution was based on the DNA content, which was determined using flow cytometry. The
648 percentage of cells in the G2/M phase was calculated. (B) CHO-K1 cells were exposed to each CDT
649 subunit at the indicated concentrations (0.01–500 nM) and incubated at 4°C for 2 h. The cells were
650 stained with individual antiserum against each CDT subunit followed by staining with
651 FITC-conjugated anti-mouse IgG. The binding activity of each CDT protein was assessed by flow
652 cytometry for FITC fluorescence. The results represent the mean and standard deviation of 3
653 independent experiments.
654
655 **FIG. 4.** Cholesterol depletion in CHO-K1 cells by treatment with MβCD. (A) CHO-K1 cells were
656 treated with 10 mM MβCD at 37°C and incubated for the indicated times. The cells were harvested and
657 subjected to cold-detergent extraction using 1% Triton X-100, followed by centrifugation to isolate the
658 DRM fraction. The prepared total cell lysates and DRM fraction were then analyzed for cholesterol
659 concentration as described in the MATERIALS AND METHODS. (B) CHO-K1 cells were treated with
660 various concentrations of MβCD (0, 2.5, 5, 10, and 20 mM) for 1 h. Whole cell lysates and the DRM

fraction were then prepared for cholesterol level analysis. (C) Cell viability was barely influenced after treatment with 0–20 mM MβCD, as determined by the trypan blue exclusion assay. The data represent the mean and standard deviation of 3 independent experiments. An asterisk indicates $P < 0.05$ compared to each untreated control group, as determined by Student's *t*-test. DRM, detergent-resistant membrane; MβCD, methyl-β-cyclodextrin.

FIG. 5. Sufficient cellular cholesterol is essential for CdtA and CdtC binding to CHO-K1 cells. The cells were untreated (upper panel) or treated (lower panel) with 10 mM MβCD for 1 h at 37°C, followed by exposure to 200 nM of the individual recombinant *C. jejuni* CDT proteins. After incubation with the individual CDT proteins for 2 h at 4°C, the cells were stained with control pre-immune serum or individual antiserum against each CDT subunit and stained with FITC-conjugated anti-mouse IgG. Binding activity was assessed by flow cytometry. The numbers represent the mean channel fluorescence (MCF). The quantitative data represent the mean and standard deviation of 3 independent experiments and are shown in the lower right panel. Statistical analysis was calculated using Student's *t*-test when compared to each untreated MβCD group. $*P < 0.05$ was considered to indicate statistical significance.

FIG. 6. Depletion of cholesterol reduces CDT holotoxin binding to cells. CHO-K1 cells were untreated (upper panel) or treated (lower panel) with 10 mM MβCD for 1 h at 37°C prior to incubation

680 with CDT holotoxin (200 nM). After incubation for 2 h at 4°C, the cells were probed with control
681 pre-immune serum or individual antiserum against each CDT subunit and stained with
682 FITC-conjugated anti-mouse IgG. The level of binding activity was analyzed by flow cytometry for
683 FITC fluorescence. The results represent the mean and standard deviation of 3 independent experiments.
684 The lower right panel shows the quantitative data of the CDT binding activity. An asterisk indicates *P*
685 < 0.05 compared to each untreated MβCD group, as determined by Student's *t*-test.
686
687 **FIG. 7.** CdtA and CdtC are enriched in detergent-resistant membrane (DRM) fractions. CHO-K1
688 cells were untreated or treated with 10 mM MβCD for 1 h prior to incubation with *C. jejuni* CDT
689 holotoxin (200 nM) for 2 h at 37°C. The cells were then subjected to cold-detergent extraction using
690 1% Triton X-100, followed by centrifugation to separate the DRM and detergent-soluble (S) fractions.
691 (A) Each fraction was subjected to western blot analysis using antibodies against caveolin-1 and CD71,
692 and individual antisera specific to CdtA, CdtB, and CdtC. The results are representative for 1 of 3
693 independent experiments. (B) The protein expression levels were analyzed using scanning densitometry.
694 The protein expression levels represent the relative distribution (%) of each protein within the DRM
695 and soluble fractions. MβCD, methyl-β-cyclodextrin.
696
697 **FIG. 8.** Association of CdtA and CdtC with membrane rafts. CHO-K1 cells were exposed to
698 medium alone or 200 nM of each recombinant *C. jejuni* CDT subunit at 11°C for 1 h. The cells were

699 washed and treated with control pre-immune serum or each anti-CDT antiserum, and then probed with
700 FITC-conjugated anti-mouse IgG (green). The cells were co-stained with anti-caveolin-1 and Alexa
701 Fluor 647-conjugated anti-rabbit IgG to visualize the raft microdomains (red) and analyzed by confocal
702 microscopy. The co-localization of each CDT subunit with lipid raft domains appears as yellow in the
703 overlay. Scale bars, 10 μm. The distribution of fluorescence intensity for each CDT subunit and Cav-1
704 signals across the blue lines were calculated and presented as line intensity histograms in the right
705 panels. Cav-1, caveolin-1.
706
707 **FIG. 9.** Localization of CdtB in membrane rafts through the association of CdtA and CdtB with
708 rafts. CHO-K1 cells were exposed to 200 nM CDT holotoxin for 1 h at 11°C. The cells were washed
709 and stained with each anti-CDT antiserum and then probed with FITC-conjugated anti-mouse IgG
710 (green). The cells were co-stained with anti-caveolin-1 and Alexa Fluor 647-conjugated anti-rabbit IgG
711 to visualize the raft microdomains (red). The stained cells were then analyzed using a confocal
712 microscope. Scale bars, 10 μm. The distribution of fluorescence intensity for individual CDT subunits
713 and Cav-1 signals across the blue lines were calculated and presented as line intensity histograms in the
714 lower panels. Cav-1, caveolin-1.
715
716 **FIG. 10.** Depletion of cholesterol prevents the nuclear localization of *C. jejuni* CdtB. (A) CHO-K1
717 cells were untreated or treated with 10 mM MβCD for 1 h prior to exposure to 200 nM CDT holotoxin

718 at 37°C for the indicated times. The cells were washed and probed with anti-CdtB antiserum, followed
719 by staining with FITC-conjugated anti-mouse IgG. The stained cells were then analyzed by confocal
720 microscopy. Scale bars, 10 μm. (B) The nuclear fraction from cell lysates was prepared from CHO-K1
721 cells untreated or treated with 10 mM MβCD for 1 h, followed by incubation at 37°C in the presence of
722 CDT holotoxin for the indicated times. CdtB in the nucleus of cell lysates was detected by western
723 blotting. The results represent 3 independent experiments. PCNA was used as a loading control for the
724 nuclear fraction of cell lysates. (C) Protein expression levels were analyzed using scanning
725 densitometry. The lower right panel shows the quantitative data for the nuclear CdtB signal. An asterisk
726 indicates $P < 0.05$ compared to each untreated MβCD group, as determined by Student's *t*-test. MβCD,
727 methyl-β-cyclodextrin; PCNA, proliferating cell nuclear antigen.
728
729 **FIG. 11.** Sufficient cellular cholesterol is essential for *C. jejuni* CDT-induced cell-cycle arrest.
730 CHO-K1 cells were pre-exposed to medium alone (A, D, and E), 5 mM MβCD (B and F), 10 mM
731 MβCD (C and G), or treated with 10 mM MβCD and replenished with cholesterol (400 μg/mL) for 1 h
732 at 37°C (H). The cells were then incubated for 48 h at 37°C in the presence of medium (A), ICRF-193
733 (D), and *C. jejuni* CDT holotoxin (E–H). The cell-cycle distribution was based on the DNA content,
734 which was analyzed with flow cytometry. The percentage of cells in the G0/G1, S, and G2/M phases of
735 the cell cycle are indicated at the right of each histogram. (I) The percentage of cells in the G2/M phase
736 were calculated and plotted as intensity histograms. The results represent 3 independent experiments.

737 *P < 0.05 was considered to indicate statistical significance. MβCD, methyl-β-cyclodextrin; Chol,
738 cholesterol.
739
740 **FIG. 12.** Cholesterol is important for CDT association and intoxication of cells. (A) Cells from the
741 indicated lines were untreated or treated with 5 mM (for AGS cells) or 10 mM (for other cells) of
742 MβCD for 1 h at 37°C, followed by exposure to 200 nM of CDT holotoxin for 48 h. Cell cycle
743 distribution was analyzed using flow cytometry. (B) Cells from the indicated lines were untreated or
744 treated with 5 mM (AGS cells) or 10 mM (other cells) of MβCD for 1 h at 37°C, followed by
745 incubation with the individual CDT proteins for 2 h at 4°C. The binding activity of each CDT protein
746 was assessed by flow cytometry for FITC fluorescence. The results represent the mean and standard
747 deviation of 3 independent experiments. An asterisk indicates P < 0.05 compared to each untreated
748 MβCD group, as determined by Student's *t*-test.
749
750 **FIG. 13.** Identification of CRAC-like region in CdtA and CdtC. Deduced amino acid sequences of
751 CdtA (upper panel) and CdtC (lower panel) are shown. The predicted amino acid motifs containing the
752 putative CRAC-like region are boxed. Numbers indicate the positions of the amino acid residues at
753 each end of the motif. Residues in gray represented conserved pattern in CRAC-like region.
754

FIG. 1

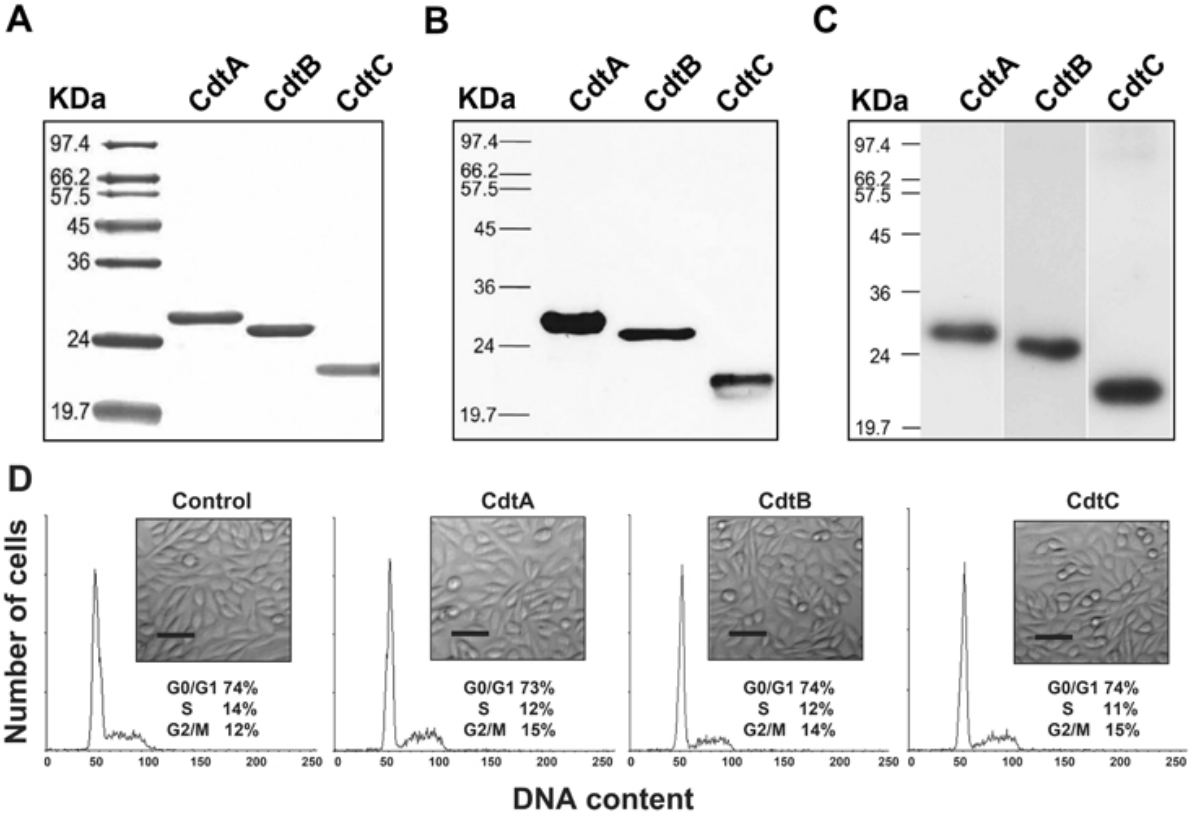

FIG.2

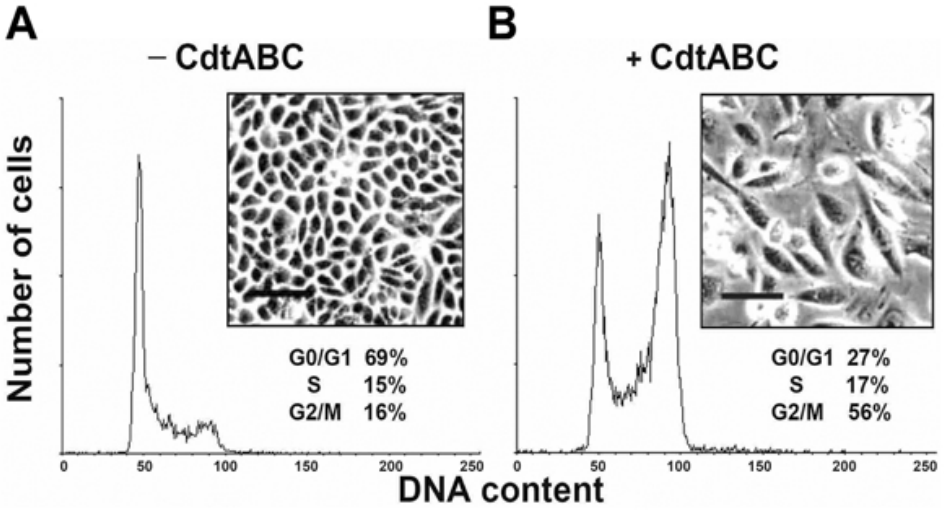

FIG. 3

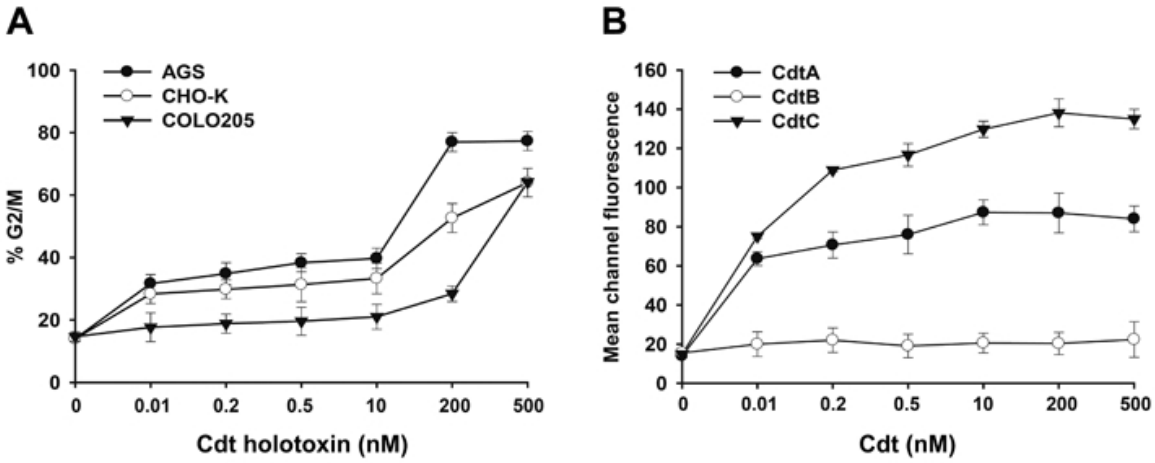

FIG. 4

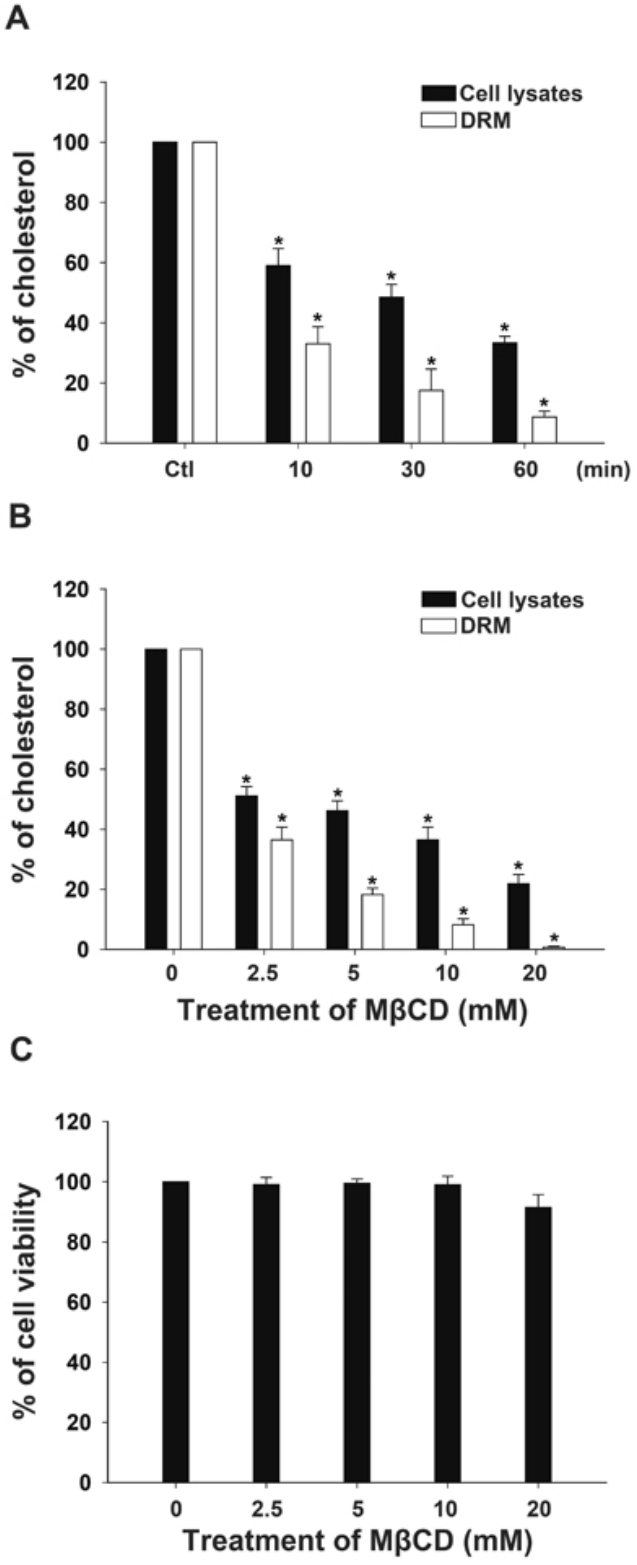

FIG. 5

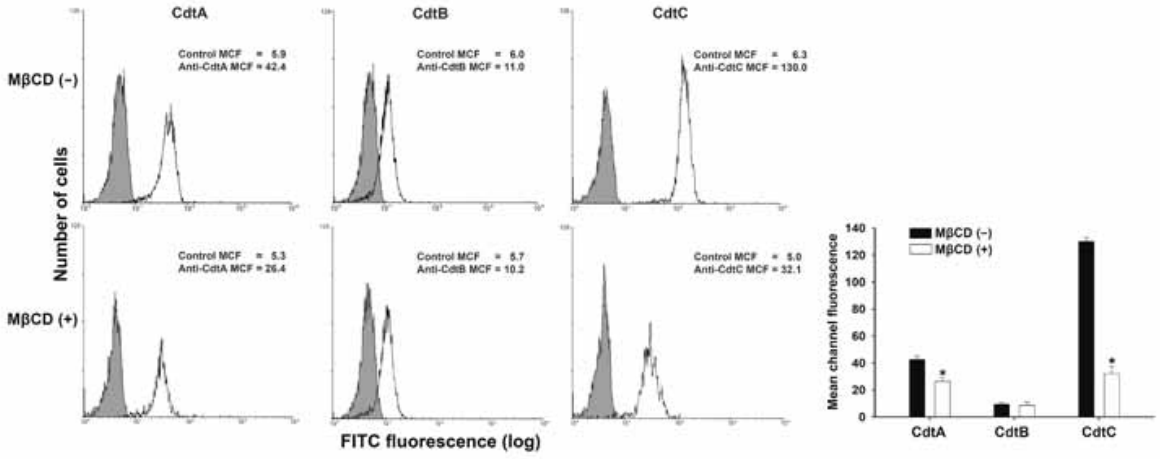

FIG. 6

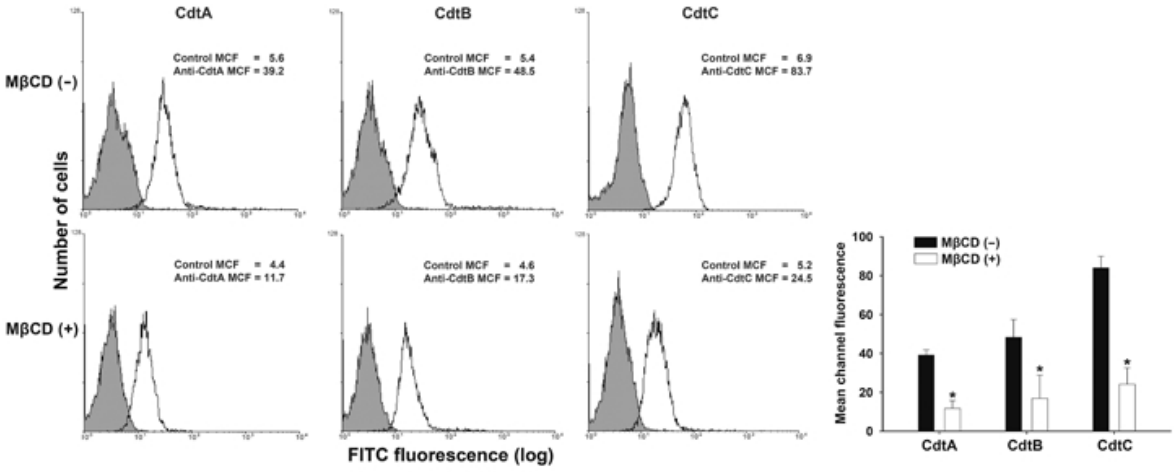

FIG. 7

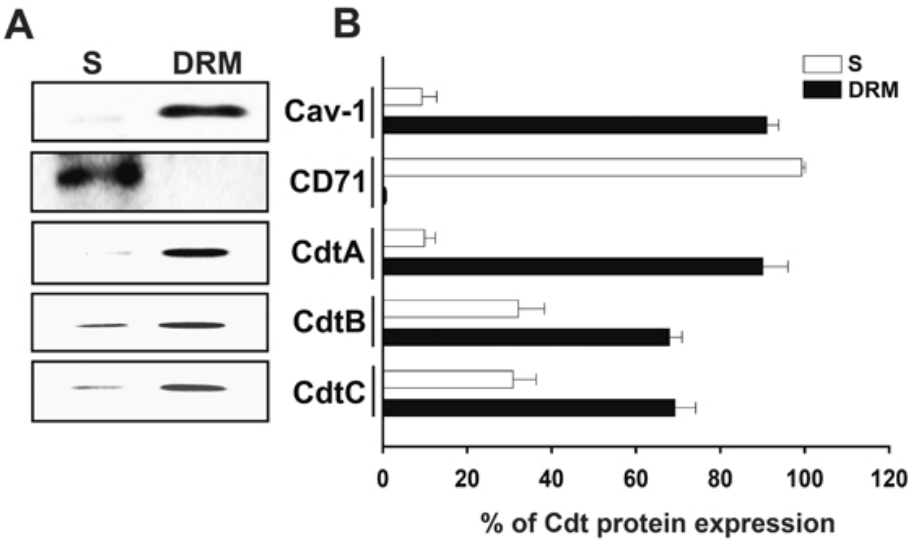

FIG. 8

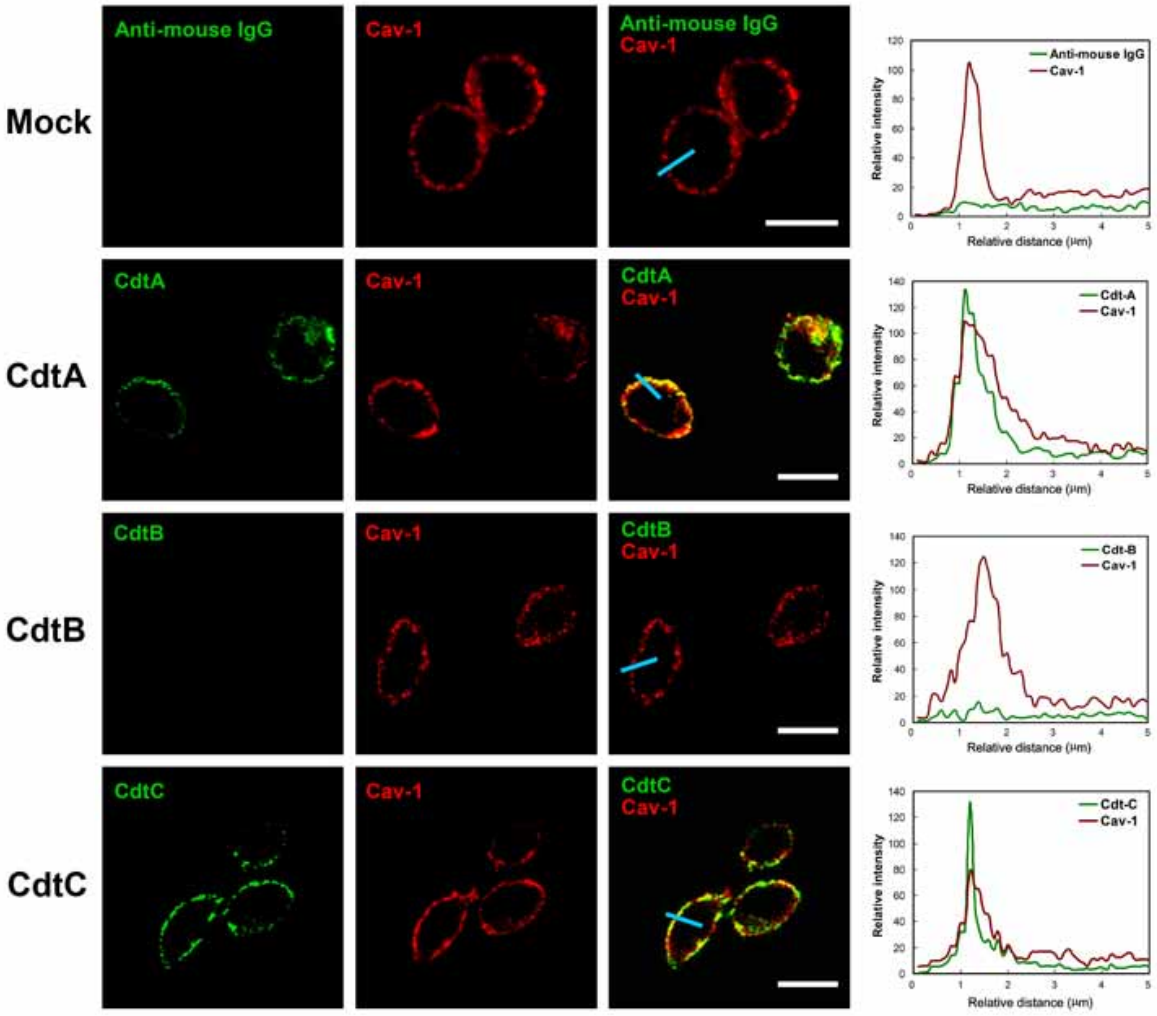

FIG. 9

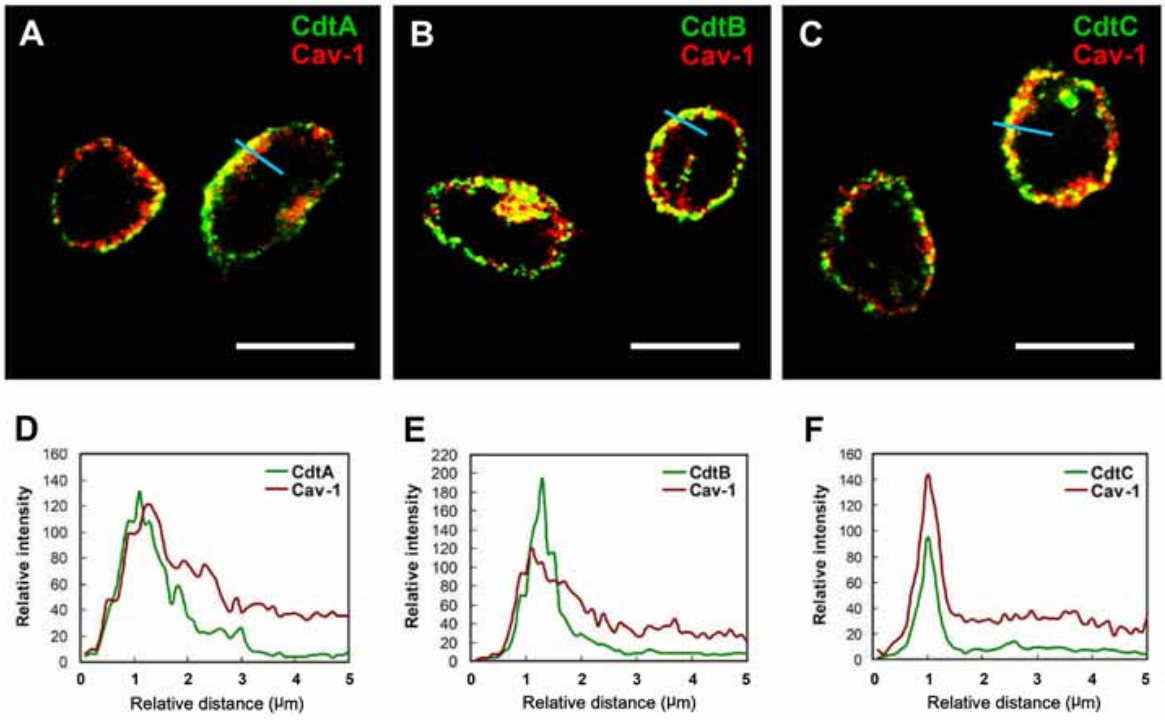

FIG. 10

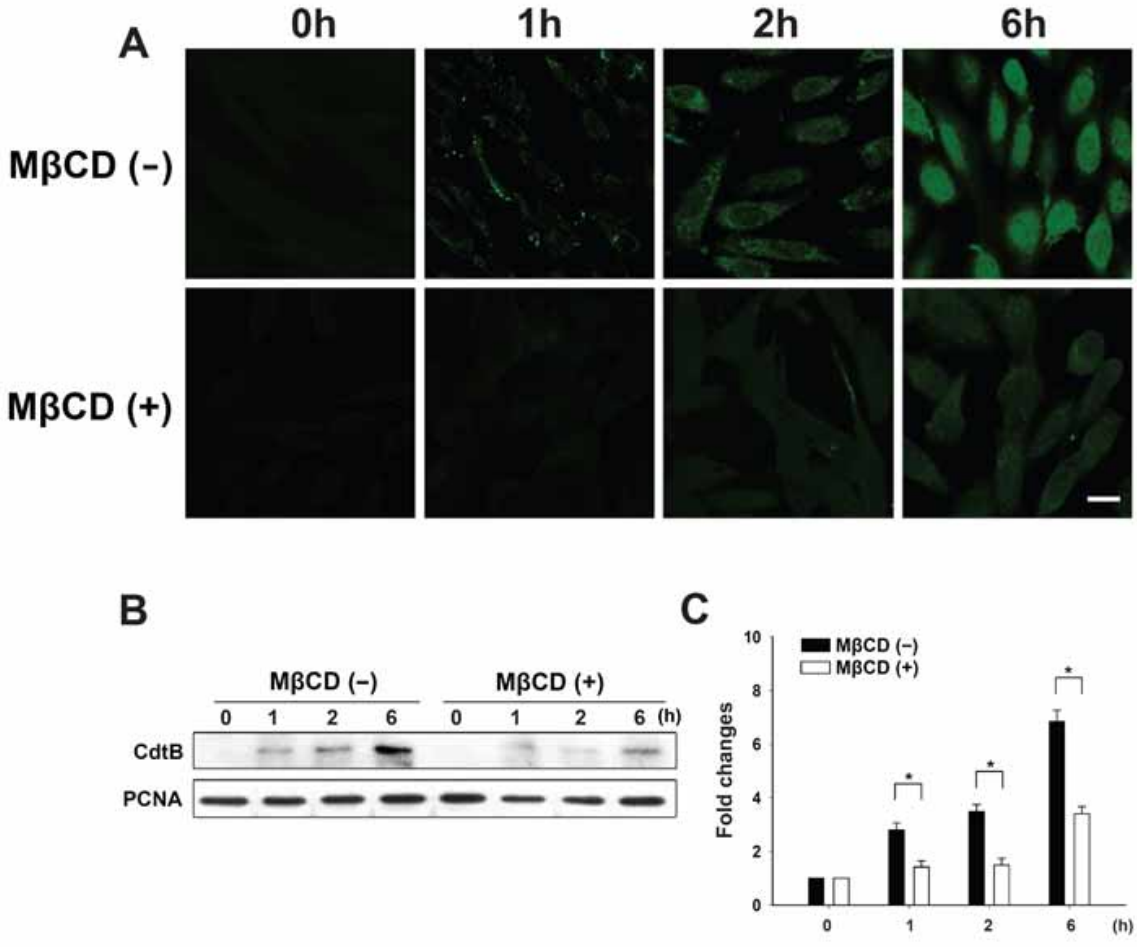

FIG. 11

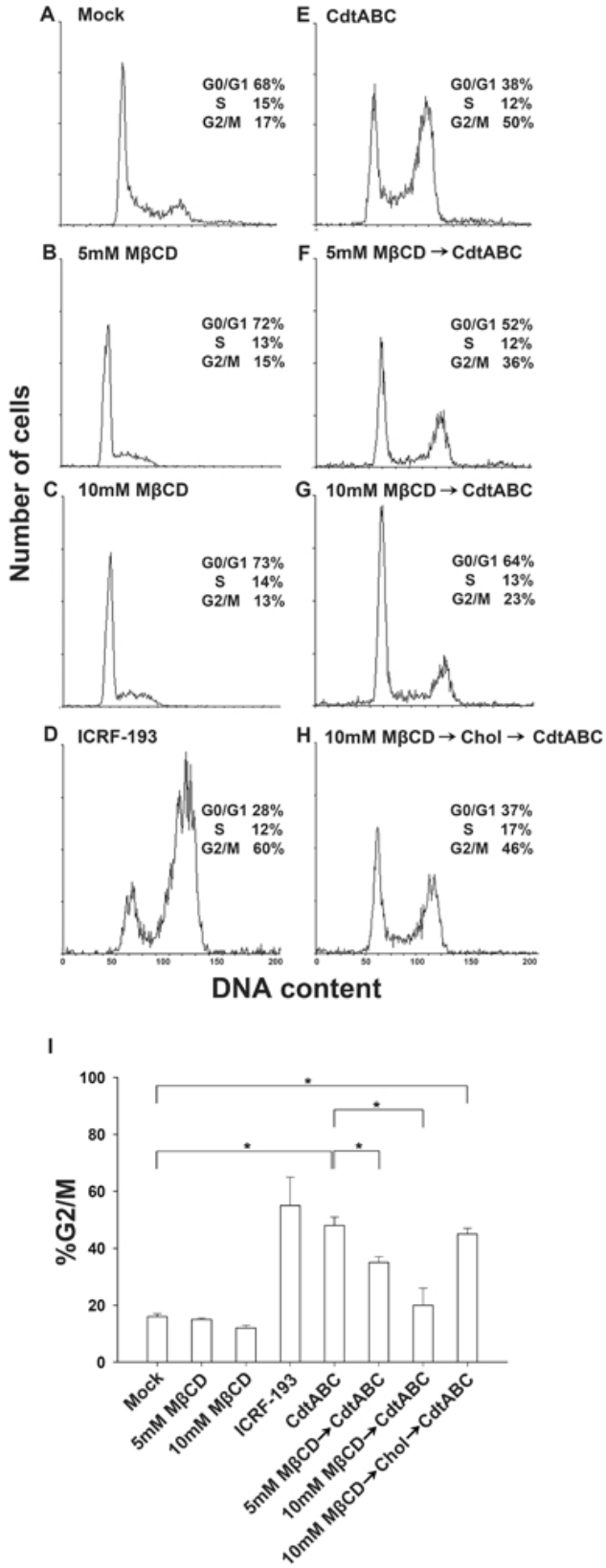

FIG. 12

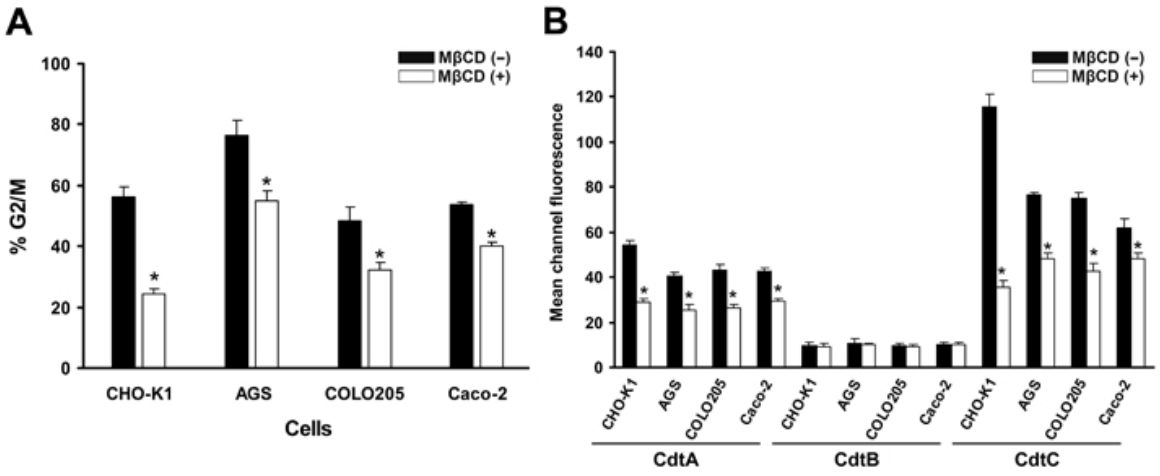

FIG. 13

Cdt A amino acid sequence

MQKIIVFILCCFMTFF[17]LY**ACSS**K[23]FENVNPLGRSFGEFEDTDPLKLGLEPTFPTNQEIPSLISGADLV
PITPITPPLTRTSNSANNNAANGINPRFKDEAFNDVLIFENRPAVSDFLTILGPSGAALTVWALAQGNW
IWGYTLIDSKGFGDARVWQLLLYPNDFAMIKNAKTNTCLNAYGNGIVHYPCDASNHAQMWKLIPMSNTA
VQIKNLGNGKCIQAPITNLYGDFHKVFKIFTVECAKKDNFDQQWFLTTPPFTAKPLYRQGEVR

Cdt C amino acid sequence

MKKIITLFFMFITLAFATPTGDLKDFTEMVSIRSLETGIFLSAFRDTSKDPIDQNWNIKEIVLSDELKQ
KDKLADE[77]L**PFGYVQFTNP**K[88]ESDLCLAILEDGTFGAKSCQDDLKDGKLETVFSIMPTTTSAVQIRSLV
LESDECIVTFFNPNIPIQKRFGIAPCTLDPIFFAEVNELMIITPPLTAATPLE